

Effect of the precursor graphite on the structure and morphology of graphite oxide and reduced graphene oxide

Demudu B. Dommisa, Raj K. Dash*

School of Engineering Sciences and Technology University of Hyderabad, Hyderabad, TS, 500046, India

*Corresponding Author, Tel: 040-2313-4460; E-mail: rkdse@uohyd.ernet.in

Received: 11 November 2016, Revised: 10 December 2016 and Accepted: 20 December 2016

DOI: 10.5185/amlett.2017.1486

www.vbripress.com/aml

Abstract

In this work the effect of the precursor graphite on the structure and morphology of the graphene oxide and reduced graphene oxide are investigated by considering three different sizes source graphite such as 2-15, <45 and 170-840 μ m respectively. All the three graphite were oxidized by Modified Hummer's method and further reduced by hydrazine hydrate by maintaining same synthesis conditions. The results demonstrated that the oxidation process is size dependent of the source graphite. The results revealed that smaller size graphite is fully oxidised as compared to larger sizes and also functionalized more. Few layers (less than 4-5) crystalline, less disorder and unfolded reduced graphene oxides are obtained when smallest size graphite is used as the source material. The water molecules present in the graphene oxide synthesised from larger size graphite as source material are higher and that can lead to the the occurrence of polycrystalline in structure, more disorder and wrinkled or folding reduced graphene oxide. Therefore, this study can open a new pathway to synthesis more crystallinity, less disorder and wrinkled free or unfold reduced graphene oxide for several potential applications. Copyright © 2017 VBRI Press.

Keywords: Size effect, modified hummer's method, graphene oxide (GO), reduced graphene oxide (RGO).

Introduction

Graphene is a 2D nanomaterial having a lot of potentials for future applications in electronics devices, MEMS, NEMS, sensors, biomedical devices due to its excellent electrical, optical and mechanical properties [1-6]. There are several methods to produce such 2D materials such that mechanical exfoliation [7], chemical exfoliation [8], thermal decomposition on SiC [9], and chemical vapor deposition [10]. However, out of all these methods, chemical rout method is more cost effective, mass production, high yield and easy production. The quality of graphene generally depends on the characteristic of the parent graphite [11], the oxidation method [12] and reduction process [13-15]. It was recently reported that the parent graphite size influence both the graphite oxide and reduce graphene oxide structure [11, 15]. However, such size dependent of source graphite on the formation of graphene oxide and reduced graphene oxide was reported by using the Modified Brodie's method and considering the 20, 74 and 149 μ m parent graphite sizes [15]. Moreover, the effect of source graphite having very smaller sizes or very larger sizes on the structure, morphology of the

graphite oxide and reduce graphene oxide synthesized by Modified Hummer's method was not reported as per our knowledge. Therefore, in this present study, the effect of three different sizes source graphite such as 2-15, <45 & 170-840 μ m on the oxidation of graphite to graphene oxide by using well known Modified Hummer's method is reported. The structure, morphology and disorder are analyzed by X-ray diffraction (XRD), Transmission Electron Microscopy (TEM), Field Emission Electron Microscopy (FESEM), Raman, TGA, FTIR and UV spectroscopy respectively to understand the effect of precursor graphite sizes on the structure and morphology of the graphene oxide and reduced graphene oxide. Experimental results revealed that source graphite size has predominant effect on the oxidation of the graphite and larger size graphite are partially oxidized whereas smaller sizes graphite is fully oxidized. Further, the water molecules present in the graphene oxide synthesised from larger size graphite as source material are higher and that can lead to the the occurrence of polycrystalline in structure, more disorder and wrinkled or folding reduced graphene oxide as compared to smaller size source graphite synthesized graphene oxide.

Experimental

Materials/ chemicals details

Graphite powders and flakes ($\geq 99.99\%$ Sigma-Aldrich) were procured having a particle size of 2-15 μm for smaller graphite, $\leq 45 \mu\text{m}$ intermediate size and 170-840 μm for a larger size. Sodium Nitrate (NaNO_3 , 99.0% Sigma-Aldrich), potassium permanganate (KMnO_4 , 99.5% Merck) and concentrated sulphuric acid (abt. 98%), hydrogen Peroxide (30%) chemicals were purchased from known vendors.

Material synthesis

Graphite oxide was synthesized from the graphite powder having their different sizes such as 2-15, <45 & 170-840 μm respectively by using the Modified Hummer's method [8] as compared to other sizes as reported in **Table 1**. In a typical experiment, 4gm of graphite(2-15 μm) powder was first added to 92 ml of concentrated H_2SO_4 and then 2g of NaNO_3 taken in the 2000ml beaker in an ice bath and stirred for 30min. Under the stirring condition, the mixture was cooled to 5 $^\circ\text{C}$ using an ice bath. The second step, KMnO_4 (12 gm) was then gradually added under cooling and stirring, within 45minutes and also the temperature was kept below 5 $^\circ\text{C}$. After this step, the ice bath was removed and once again stirring for 1h at RT on the hot plate till the temperature reached 35 $^\circ\text{C}$ with continuing the stirring for additional 4h. Further the temperature was increased from 35 $^\circ\text{C}$ to 100 $^\circ\text{C}$ and at this stage 184 ml of DI water was added by continuing the stirring for 15min. Then the mixture solution was diluted in approximately 560ml with DI water. Next step, 40 ml of 30% H_2O_2 was added to the mixture to reduce the residual KMnO_4 present in the mixture solution. The mixture solution was washed many times with the DI water and then 35% HCl was added until pH value reached to 7. The obtained graphite oxide (GO) was collected by centrifuging, vacuum filtering and drying process. Finally, the resulting graphite oxide (GO) was dried at 60 $^\circ\text{C}$ for 12 h in an oven. Same process as mentioned above was carried out for other two sizes graphite i.e. <45 and 170-840 μm by maintaining the

same parameters to investigate the source graphite powder size effect on the formation of the graphene oxide. For reduction of graphite oxide to reduced graphene oxide, 250mg of the as-synthesized graphite oxide (2-15 μm) was added to 250ml DI water in a 500ml beaker and sonicated for 60minutes till obtained a clearer solution. Then hydrazine hydrate 10ml was added to the graphene oxide solution and heated at 95 $^\circ\text{C}$ with continuous stirring for almost 6hours. The whole experimental was maintained on a hotplate by using the silicon oil bath. After completion of the reaction, the material was filtered by using a vacuum pump and washed several times with the DIW till pH = 7. Finally, filtered with a standard filter paper by using the vacuum pump and dried at 60 $^\circ\text{C}$ in the Oven for 12h. The same process was also carried out for other two graphite oxide as obtained from <45 and 170-840 μm source graphite powders.

Characterizations

X-Ray diffraction (XRD) technique was used for the studying the crystallinity of the samples. XRD pattern was recorded from 5 to 40 $^\circ$ using the CuK_α as the x-ray source ($\lambda=1.54\text{\AA}$) and step size 0.02 with scan speed 0.4 $^\circ$ for all samples (model: Bruker's AXS D8 Advance system). Field Emission Scanning Electron Microscopy (FESEM, model: Zeiss Ultra55) was utilized for studying the morphology of the samples by using the secondary electrons(SE) and acceleration voltage 5KV. Transmission Electron Microscopy (TEM, Model: FEI Technai G2S-Twin) was also used for the studying the morphology and structural properties. The operating acceleration voltage of TEM was 200KV. The electron diffraction indicates the crystallinity of the samples. Raman spectroscopy (model: Witech alpha 300) was used for analyzing the structural, defects and disorder in the synthesized samples. In Raman analysis, Nd-YAG Laser of having wavelength 532nm was considered. The laser power was kept at 10% of the maximum power (40mw) in order to avoid any thermal influence in the samples to modify the structural information of the samples. The laser beam (spot size 1 μm) was focused on the samples by

Table. 1. Comparison of the present reported work with previously reported work.

S. no.	Graphite Sources	Size of Graphite Sources	Method	Reference
1	Natural graphite	20,74,149 μm	Modified Brodie method	[15]
2	Natural graphite	<45 μm	Modified Hummer's method	[22]
	Synthetic	<20 μm	Standen maier's method	
3	Flakes Ground Powders	NA	Modified Hummer's method	[23]
4	Natural graphite	80-120mesh, 750-850 mesh, 2000mesh	Modified Hummer's method	[24]
5	Natural graphite	80mesh,50mesh,35mesh	Expanded graphite	[25]
6	Natural graphite	-200mesh,-100mesh, +150mesh, +50mesh,	Modified Hummer's method	[26]
7	Powders	2-15 μm , <45 μm , 170-840 μm	Modified Hummer's method	Present work

means of a confocal microscope and 100x objective and also the spectrum range from 500-4500 cm^{-1} . The bonding characteristics, functional groups present in the samples were analyzed by Fourier Transformation Infra-Red spectroscopy (FTIR, modal: Perkin Elmer) by using the KBr pellets in the range 500-4000 cm^{-1} . UV spectrometer (modal: Jasco U-670) was used for to measure the optical absorption properties of samples in the range of 200nm to 850nm. A thermogravimetric analyzer (TGA) was used to determine the thermal stability of samples under nitrogen flow condition with 10 $^{\circ}\text{C}$ / minute heating rate.

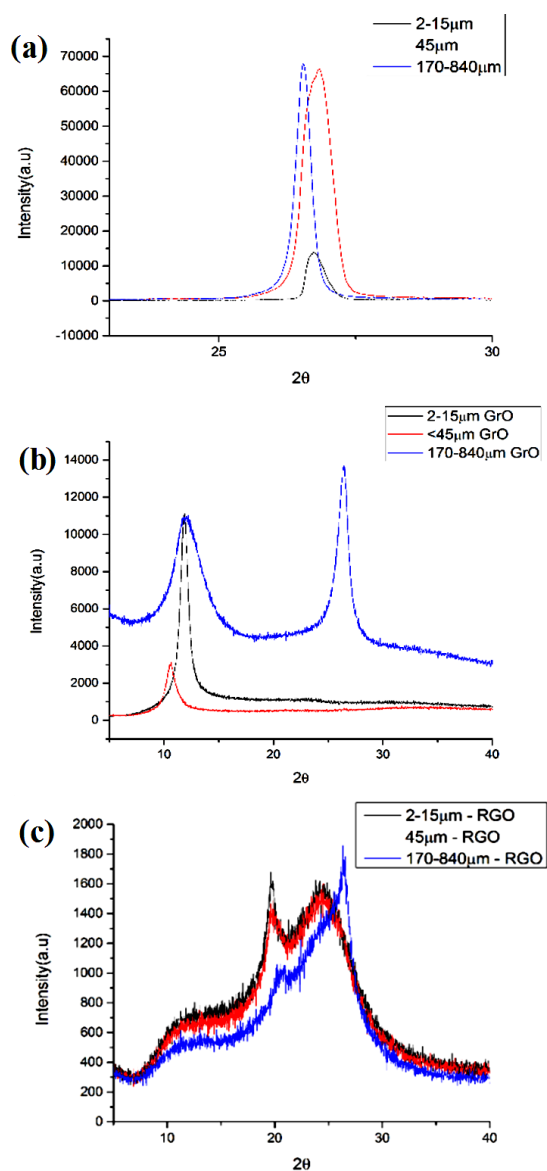


Fig. 1. XRD pattern of (a) different sizes of graphite powder such as 2-15, <45 and 170-840 μm . (b) shows the graphite oxide (GO) of 2-15, <45 and 170-840 μm and (c) shows the RGO of 2-15, <45 and 170-840.

Results and discussion

Fig. 1(a) shows the XRD pattern of source graphite powders having three different sizes i.e. 2-15, <45 and 170-840 μm and all the three graphite powders

showing the peak nearly at $2\theta=26.6^{\circ}$. The corresponding inter planar distance(d) is near to 3.3 \AA for all the graphite powders and among all 170-840 and <45 μm graphite has more intensity than 2-15 μm because of bigger size [15]. The crystallite sizes are obtained by using the XRD data and are 21.3nm, 13.5nm and 24.7 for 2-15, <45 and 170-840 μm graphite powders respectively. **Fig. 1(b)** shows the XRD spectrum after oxidation of all the three graphite powders and the inter planar distance(d) increases to 7.1 ,7.7 and 7 \AA for graphite oxide from the parent graphite having sizes 2-15, <45 and 170-840 μm respectively. The increase in the inter planar distance (d) for all the three-graphite oxide confirm the intercalation of water molecules and oxygen functional groups between graphite layers. However, in the case of graphite oxide synthesized from 170-840 μm size graphite has another peak $2\theta = 26.4^{\circ}$ having $d = 3.4\text{\AA}$, which indicates the 170-840 μm is partially oxidized.

Therefore, bigger size graphite is not fully oxidized under this conditions and hence the oxidation process of graphite is size dependent i.e. the smaller size of graphite is fully oxidized within 4 hours' time of reaction whereas bigger size (170-840 μm) graphite need more time or a different ratio of chemicals to fully oxidized. Also after oxidation, smaller size source i.e. 2-15 μm graphite oxide has more intensity peak than other two sizes. Therefore 2-15 μm size graphite oxide has more crystallite sizes than other two sizes. **Fig. 1(c)** shows the XRD spectrum after reduction of graphite oxide for all the three-graphite oxide. It is seen that the inter planar distance(d) decreases from 7.5 \AA to 4.5 \AA of all samples, which indicates the oxygen functional groups are subsequently removed and broad peak represent that smaller crystallites are formed. Also, a small pump is noticed at 19-20 $^{\circ}$ (as shown in **Fig. 1(c)**) indicates some functional groups are present between the carbon back bone after reduction process or another phase may be present in the RGO [21].

Fig. 2(a)-(c) show the TEM images of all three graphite oxides. It is observed from **Fig. 2(a)** that less folding and disorder are present in the smaller size graphite synthesized graphene oxide as compared to larger sizes source graphite synthesized graphene oxide. More thick sheet morphology and less transparency are observed for the graphene oxide synthesized by using the 170-840 μm graphite as compared to smaller size graphite powder synthesized graphene oxide. From, SAED pattern, the hexagonal structure of two rings are observed and HRTEM clearly shows the lattice fringes <4 layers for 2-15 μm graphene oxide. Clearly diffraction spots indicate the characteristic of crystalline order which is also supported by XRD results. **Fig. 2(b)** shows the SAED pattern for the second sample (< 45 μm). It is confirmed that ring like diffraction pattern which indicates the polycrystalline nature of GO (as shown in **Fig. 2(b)**). HRTEM image (**Fig. 2(b)**) clearly shows more

folding of lattice fringes of GO. The third sample (170-840 μm) SAED and HRTEM (**Fig. 2(c)**) confirm the multi layers nature of GO because of partially oxidized. **Fig. 2(d)** shows the TEM image of 2-15 μm RGO and confirms the reduced graphene oxides are having less folding, flat sheet and more transparent in nature.

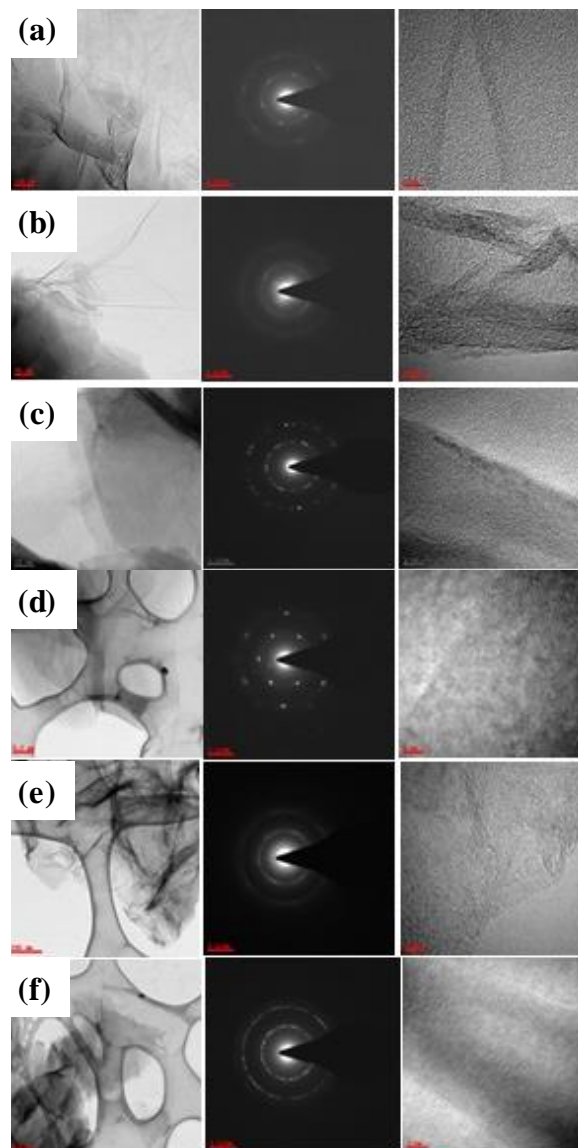


Fig. 2. TEM images (a), (b) and (c) are 2-15, <45 and 170-840 μm graphene oxide corresponding SAD and HRTEM images and (d), (e) and (f) are corresponding 2-15, <45 and 170-840 μm reduced graphene oxide SAD and HRTEM images respectively.

The SAED pattern shows the sharp diffraction spots which further indicates the restoration of sp^2 hybridized carbon atoms by the chemical reduction. HRTEM image clearly confirms <3-4 layers are present in the sample. **Fig. 2(e)** shows the TEM image of <45 μm RGO, which clearly shows more folding with transparency in nature and SAED pattern confirms very fewer intensity spots with hexagonal structure. Moreover, the HRTEM image confirms even having single layer lattice fringes which are distributed randomly. **Fig. 2(f)** shows the

TEM images of 170-840 μm RGO and it is seen from **Fig. 2(e)** that thick sheet is present in the corresponding RGO and SAED pattern clearly confirms diffraction spots of multilayer formation. Therefore, TEM results correlate with the corresponding XRD results and conclude that after oxidation and reduction smaller size graphite synthesized reduced graphene oxide has good crystallinity and less folding as compared to that of bigger sizes graphite powders. **Fig. 3(a)** shows the Raman spectrum of 2-15, <45 and 170-840 μm as source graphite synthesized graphene oxide. It is seen from **Fig. 3(a)** that for all the three GO samples, D band appears at 1354, 1353 and 1355 cm^{-1} and G band at 1590, 1585 and 1585 cm^{-1} respectively. Also, the I_D/I_G ratio are 0.95, 0.88 and 0.78 for corresponding 2-15, <45 and 170-840 μm graphene oxide respectively. The broad and the peak shift to the higher wavenumber of G band along with the increases in the I_D/I_G ratio GO samples are better oxidation [17]. Therefore 2-15 μm graphene oxide is better oxidized as compared to larger size source graphite i.e. <45 and 170-840 μm corresponding GO samples. **Fig. 3(b)** shows the Raman spectrum of 2-15, <45 and 170-840 μm reduced graphene oxide (RGO) respectively.

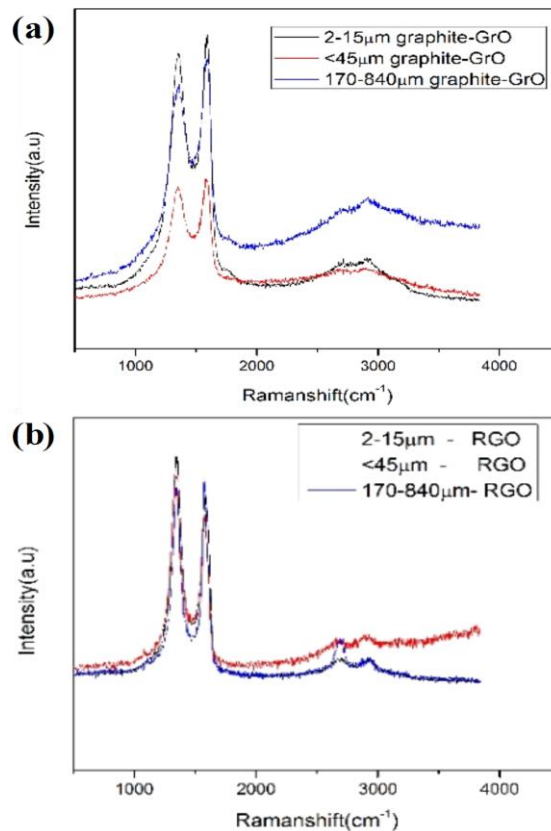


Fig. 3. Raman spectra of (a) 2-15, <45 and 170-840 μm graphite oxides and (b) 2-15, <45 and 170-840 μm reduced graphene oxides respectively.

The D band appears at 1348, 1342 and 13146 cm^{-1} and corresponding G band at 1586, 1576 and 1580 cm^{-1} for 2-15, <45 and 170-840 μm reduced graphene oxide (RGO) respectively. The I_D/I_G ratios are 1.32,

1.26 and 0.99 for 2-15, <45 and 170-840 μm reduced graphene oxides respectively. After reduction, the I_D/I_G ratio increases as compare to only oxidation of the graphite, which indicates that the new created graphitic domain in RGO is more numerous in number than that presented in the GO i.e. size of the sp^2 domain in GO decreased after chemical reduction. Since, 2-15 μm RGO has more I_D/I_G ratio comparative other two samples, the smaller size graphite has more formation of new sp^2 domains after chemical reduction. This result may be consistent with the XRD results i.e. formation of the broad peak in XRD after reduction. **Fig. 4(a)** shows the FTIR spectrum of 2-15, <45 and 170-840 μm as source graphite corresponding graphite oxides. All three samples have similarly peak positions of functional groups with very small variation in the intensity and broad peaks [18]. All the three samples contain the functional groups at 3400cm^{-1} of O-H stretching vibration of the hydroxyl groups and intercalated water molecules between graphite layers. 1724cm^{-1} indicates the C=O stretch mode in the carbonyl groups, 1620cm^{-1} contributes to the C=C skeletal vibration of an oxidized graphitic domains or contribution from the stretching deformation of O-H vibration of intercalated water, 1380cm^{-1} indicates the OH deformation vibration of COOH groups, 1228cm^{-1} attributes to the C-O stretching peak of epoxy groups and 1051cm^{-1} indicates the C-O group of alkoxy of stretching vibration mode. All three samples attributed broad and more intensity peaks observed of hydroxyl and epoxy groups and fewer intensity peaks are observed for carbonyl and carboxyl groups i.e. large amount of hydroxyl and epoxy groups distributed on the basal plane of the GO and less amount of carboxyl and carbonyl groups formed at edges of GO sheets.

During the graphite oxidation process, oxygen functional groups such as epoxy, hydroxyl, carbonyl and carboxyl are heavily decorated on the plane of the carbon atoms. Out of those oxygen functional groups both the epoxy and hydroxyl groups are located on the basal plane of GO and these are major components. However, both the carbonyl and carboxyl groups are minor groups and are mostly located at the edges of the GO [27,28]. **Fig. 4(b)** shows the FTIR spectrum of 2-15, <45 and 170-840 μm reduced graphene oxides by hydrazine hydrate. It is observed from all the three samples that 1724cm^{-1} , 1228cm^{-1} and 1051cm^{-1} peaks corresponding to carbonyl, epoxy and alkoxy are absent in all the samples. It is also noticed from **Fig. 4(b)** that the broadness and intensity of 3400cm^{-1} peak i.e. hydroxyl groups decrease that may be due to the removal of these group due to partially oxidation. **Fig. 5(a)** shows the TGA spectrum of 2-15, <45 and 170-840 μm graphite oxides. As shown in **Fig 5(a)**, all the three samples lose weight at $< 100^\circ\text{C}$. The corresponding weight losses are 10.6, 11.5 and 8.3% for 2-15, <45 and 170-840 μm graphite oxides respectively. The weight losses in between 130-300 $^\circ\text{C}$ are 37.4, 32.8 and 24.4% for 2-15, <45 and

170-840 μm graphite oxides respectively. These three samples show the different percentage of weight loss and more weight loss is observed in the case of 45 μm the graphite dependent on the size of the source graphite. At $<100^\circ\text{C}$, the water molecules evaporation takes in graphite oxide, which indicates that the oxidation of place [17] and between 130-300 $^\circ\text{C}$ range weight loss due to the decomposition of the oxygen containing functional groups such as yielding CO, CO_2 and steam [17,19].

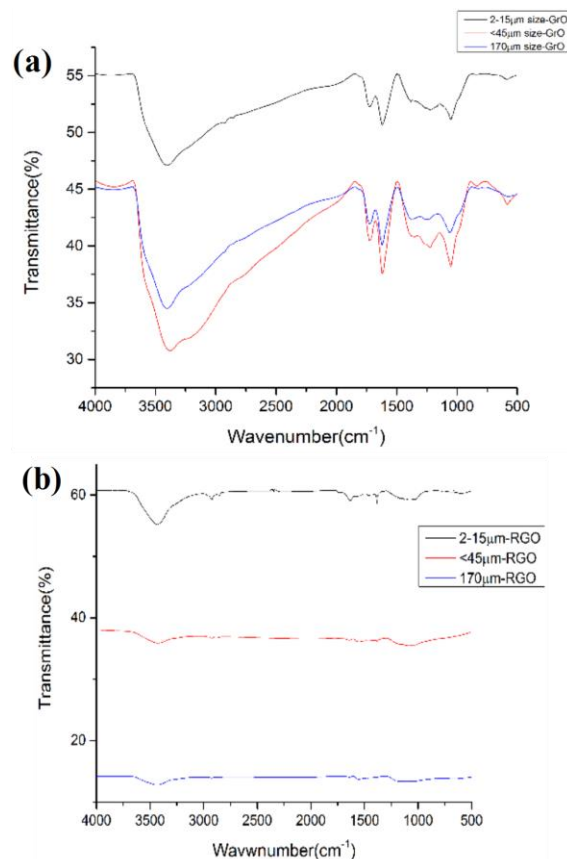


Fig. 4. FTIR spectrum of (a) 2-15, <45 and 170-840 μm Graphite oxides and (b) 2-15, <45 and 170-840 μm reduced graphene oxides respectively.

It is seen from the **Fig. 5(a)** that <45 μm graphite oxide has more water molecules between the graphite layers as compare to other two sizes GO. These water molecules can attribute to more folding, polycrystalline and disorder of lattice fringes as observed in the TEM analysis and also correlated with XRD and FTIR results for GO synthesized from <45 μm source graphite. At 130-300 $^\circ\text{C}$ range more weight loss is observed in 2-15 μm graphite oxide i.e. it has more oxygen containing functional groups. Therefore, the smaller size graphite completely oxidizes as compared bigger size graphite. The disordered stacking of graphene layers and distorted microstructures are mostly obtained due to the curved graphene layers, structural defects and increased interlayer spacing [29-31]. In this work, the intercalated water molecules in the graphite oxide can be confirmed from the TGA, FTIR and

XRD experimental results. The weight loss obtained at $< 100^{\circ}\text{C}$ are 10.6, 11.5 and 8.3 for 2-15, <45 and 170-840 μm respectively as confirmed from the TGA analysis which further indicated that the water molecules are more attributed for $<45\mu\text{m}$ size graphite oxide. Further, the experimental results from the FTIR confirmed that the hydroxyl groups and water molecules are more present in the graphene oxide synthesized from the larger sizes source graphite.

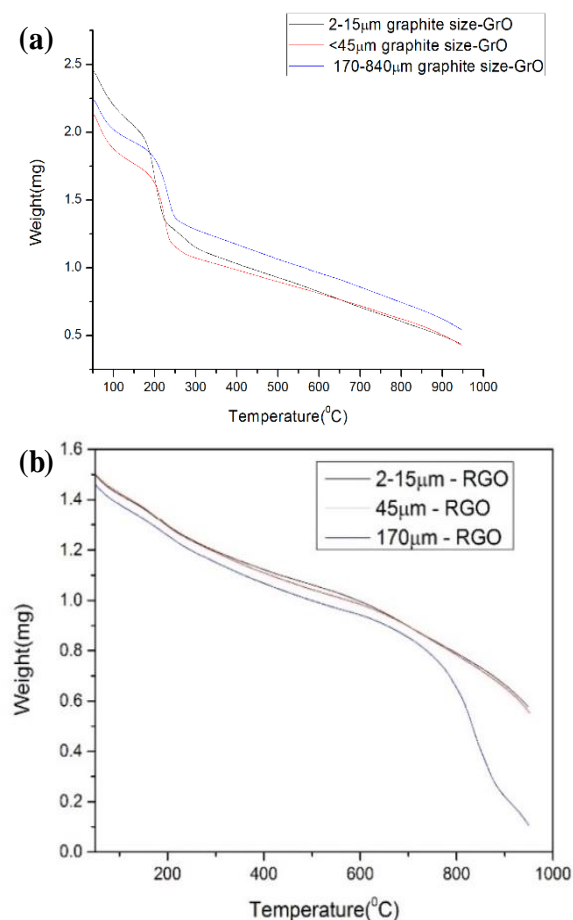


Fig. 5. TGA analysis spectrum of (a) 2-15, <45 and 170-840 μm graphite oxides and (b) 2-15, <45 and 170-840 μm reduced graphene oxides respectively.

The interlayer spacing is increased more for $<45\mu\text{m}$ size synthesized GO from the XRD analysis and which further indicated that more folding or disorder structure GO from the larger sizes source graphite. **Fig. 5(b)** shows TGA analysis spectrum of all three RGOs. As seen from the **Fig. 5(b)** that all the three samples are thermally stable i.e. there is no sudden weight loss between 130-300 $^{\circ}\text{C}$ ranges indicates the removal of oxygen functional groups. **Fig. 6(a)** shows the UV-vis spectra for 2-15, <45 and 170-840 μm graphite oxides. Two peaks are observed (**Fig. 6(a)**) in all three samples with corresponding wave lengths are 242, 249 and 263nm respectively. Such peaks are generally considered as $\pi-\pi^*$ transitions of aromatic C-C bonds and a shoulder peak at 297,310 and 305nm corresponding to the $n-\pi^*$

transition of C=O bond respectively. The above peaks around 250nm indicates the more epoxy groups are formed during the synthesis of graphite oxide [20] and the peak at 263nm indicates the electronic properties of GO with different coverage of OH and O form epoxy groups which are deeply affected by the charge distribution as well as by the formation of hydrogen bonds[20]. **Fig. 6(b)** shows the UV-vis spectra of all three RGOs and the absorption peaks are seen at 269, 270 and 270nm for 2-15, <45 and 170-840 μm as source graphite reduced graphene oxides respectively. These peaks indicate the restoration of SP^2 carbons after the reduction process.

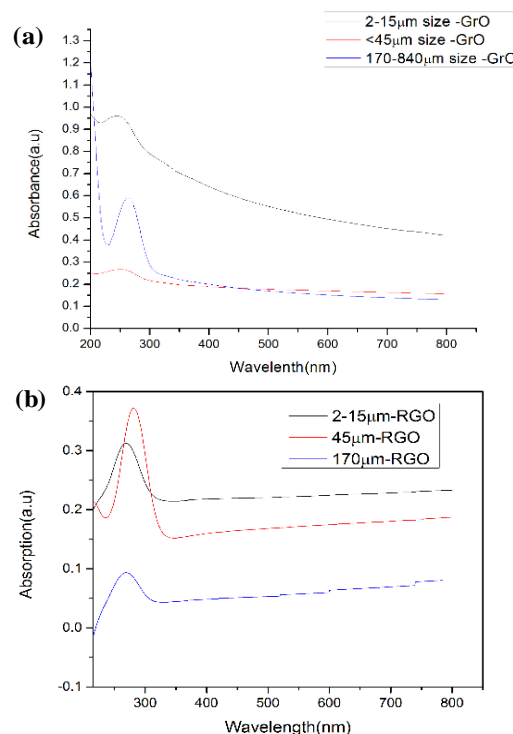


Fig. 6. UV-vis spectrum of (a) 2-15, <45 and 170-840 μm graphite oxides and (b) 2-15, <45 and 170-840 μm reduced graphene oxides.

In our experimental work, the possible mechanism to obtain unfolded, flat sheet, more crystallinity and less disorder reduced graphene oxide is that as the source graphite size become larger more water molecules are present between the graphite layers and after reduction that can possibly create folding and more disorder to restore the SP^2 carbons structure in the reduced graphene oxide as compared to those are synthesized by using very smaller source graphite powder. Hence, it may be necessary to carry out more controlled and carefully heat treatment to remove these unwanted water molecules before starting the reduction process for larger sizes source graphite powder.

Conclusion

In this present work, three different sizes graphite i.e. smaller to very larger are considered as source

materials for the synthesis of graphene oxide by using modified Hummer's method and reduction by using hydrazine hydrate. It is observed that smaller size graphite oxidized completely as compared to larger sizes under same synthesis conditions. However, larger size graphite is partially oxidized. Therefore, the oxidation of graphite is dependent on the source graphite size. It is also concluded from the XRD, TEM and Raman analysis that RGO synthesized from the smaller size graphite (2-15 μ m) are more crystallinity also showing the better quality than larger source graphite synthesized GO and RGO. Morphology of the GO and RGO of different sizes graphite after oxidation and reduction shows that RGO synthesized from the smaller size graphite has the flat surface, less folding and more transparent than that of RGO synthesized from the bigger size of graphite. TGA analysis also confirmed that the weight loss in graphite oxide is also size dependent of the source graphite powders. After reduction, all the samples showed thermal stability due to the removal of the oxygen functional groups which was confirmed from the FTIR results. All the three GO have different absorption peaks in UV-Vis spectroscopy indicated that they have different intensity of epoxy groups and also after reduction all three samples restore the sp² bond carbon atoms. Therefore, flat surface and less folding, wrinkle free reduced graphene oxide (RGO) having higher crystallinity and less disorder can be obtained by choosing the proper smaller size graphite as source material due to the removal of oxygen functional groups is more which in turn can possibly form the long ranged sp² network [32]. Such type of RGO can have the potential to use in future NEMS, Nano devices, sensors and bio-medical applications.

Acknowledgement

This work is supported by UGC startup project, UGC, India.

Author's contributions

DBD performed the experiments: Data analysis: DBS, RKD; Wrote the paper: DBD and RKD. Authors have no competing for financial interests.

References

- Geim, A.; Novoselov, K.; *Nat. Mater.*, **2007**, *6*, 183.
DOI: [10.1038/nmat1849](https://doi.org/10.1038/nmat1849)
- Lee, C.; Wei, X.; Kysar, J.; Hone, J.; *Science*, **2008**, *321*, 385.
DOI: [10.1126/science.1157996](https://doi.org/10.1126/science.1157996)
- Seol, J.; Jo, I.; Moore, A.; Lindsay, L.; Aitken, Z.; Pettes, M.; et al.; *Science*, **2010**, *328*, 213.
DOI: [10.1126/science.1184014](https://doi.org/10.1126/science.1184014)
- Berger, C.; Song, Z.; Li, X.; Wu, X.; Brown, N.; Naud, C.; et al.; *Science*, **2006**, *312*, 1191.
DOI: [10.1126/science.1125925](https://doi.org/10.1126/science.1125925)
- Tiwari, A.; Syväjärvi, M.; (Eds), In *Advanced 2D Materials*, John Wiley & Sons, Beverly, MA, USA, **2016**.
- Rao, C.; Sood, A.; Voggu, R.; Subrahmanyam, K.; *J. Phys. Chem. Lett.*, **2010**, *1572*.
DOI: [10.1021/jz200705w](https://doi.org/10.1021/jz200705w)
- Chang, Y.; Kim, H.; Lee, J.; Song, Y.; *Appl. Phys. Lett.*, **2010**, *97*, 21.
DOI: [10.1063/1.3521257](https://doi.org/10.1063/1.3521257)
- Hummers, W.; Offeman, R.; *J. of American Chemical Society*, **1958**, *80*, 1339.
DOI: [10.1021/ja01539a017](https://doi.org/10.1021/ja01539a017)
- Berger, C.; Song, Z.; Li, T.; Li, X.; Ogbazghi, A.; Feng, R.; et al.; *J. Phys. Chem. B*, **2004**, *108*, 19912.
DOI: [10.1021/jpo40650f](https://doi.org/10.1021/jpo40650f)
- Reina, A.; Jia, X.; Ho, J.; Nezich, D.; Son, H.; Bulovic, V.; Dresselhaus, S.; Kong, J.; *Nano Lett.*, **2009**, *9*, 30.
DOI: [10.1021/nl801827v](https://doi.org/10.1021/nl801827v)
- Botas, C.; Alvarez, P.; Blanco, C.; *Carbon*, **2012**, *50*, 275.
DOI: [10.1016/j.carbon.2011.08.045](https://doi.org/10.1016/j.carbon.2011.08.045)
- Dreyer, D.; Park, S.; Bielawski, C.; *Chem. Soc. Rev.*, **2010**, *39*, 228.
DOI: [10.1039/b917103g](https://doi.org/10.1039/b917103g)
- Pei, S.; Cheng, H.; *Carbon*, **2012**, *50*, 3210.
DOI: [10.1016/j.carbon.2011.11.010](https://doi.org/10.1016/j.carbon.2011.11.010)
- Parlak, O.; Turner, APF.; Tiwari, A.; *Advanced Materials*, **2014**, *26*, 482.
DOI: [10.1002/adma.201303075](https://doi.org/10.1002/adma.201303075)
- Parlak, O.; Turner, APF.; Tiwari, A.; *J. Mater. Chem. B*, **2015**, *3*, 7434.
DOI: [10.1039/C5TB01355K](https://doi.org/10.1039/C5TB01355K)
- Jeong, H.; Lee, Y.; Lahaye, R.; *J. Am. Chem. Soc.*, **2008**, *130*, 1362.
DOI: [10.1021/ja0764730](https://doi.org/10.1021/ja0764730)
- Stankovich, S.; Dikin, D.; *Carbon*, **2007**, *45*, 1558.
DOI: [10.1016/j.carbon.2007.02.034](https://doi.org/10.1016/j.carbon.2007.02.034)
- Park, S.; Lee, K.; *ACS Nano*, **2008**, *2*, 572.
DOI: [10.1021/nn700349a](https://doi.org/10.1021/nn700349a)
- Lerf, A.; He, H.; *J. Phys. Chem. B*, **1998**, *102*, 4477.
DOI: [10.1021/jp9731821](https://doi.org/10.1021/jp9731821)
- Jiang, X.; *J. Catal.*, **2013**, *299*, 204.
DOI: [10.1016/j.jcat.2012.12.022](https://doi.org/10.1016/j.jcat.2012.12.022)
- Shin, H.; Kim, K.; Benayad, A.; Yoon, S.; Park, H.; Jung, I.; Jn, M.; Jeong, H.; Kim, J.; Choi, J.; Lee, Y.; *Adv. Funct. Mater.*, **2009**, *19*, 1987.
DOI: [10.1002/adfm.200900167](https://doi.org/10.1002/adfm.200900167)
- Adriano, A.; Chun, K.; Bahareh, K.; Zdenek, S.; *PNAS*, **2012**, *109*, 12899.
DOI: [10.1073/pnas.1205388109](https://doi.org/10.1073/pnas.1205388109)
- Dhifaf, A.; Neas, L.; Kostas, K.; *2D Mater.* **2016**, *3*, 014006.
DOI: [10.1088/2053-1583/3/1/014006](https://doi.org/10.1088/2053-1583/3/1/014006)
- Haoran, Y.; Keyu, X.; Jingzhi, H.; *RSC Adv.*, **2016**, *6*, 17023.
DOI: [10.1039/c5ra24501j](https://doi.org/10.1039/c5ra24501j)
- Li, J.; Menglu, W.; *Adv. Mater. Research*, **2012**, *499*, 12.
DOI: [10.4028/www.scientific.net/AMR.499.12](https://doi.org/10.4028/www.scientific.net/AMR.499.12)
- Haiyang, X.; Tongjiang, P.; Hongjuan, S.; *Materials Science Forum*, **2015**, *814*, 185.
DOI: [10.4028/www.scientific.net/MSF.814.185](https://doi.org/10.4028/www.scientific.net/MSF.814.185)
- Xingfa, G.; Joonkyung, J.; Shigeru, N.; *J. Phys. Chem. C*, **2010**, *114*, 832-842.
DOI: [10.1021/jp909284g](https://doi.org/10.1021/jp909284g)
- Xiluan, w.; Gaoquan, S.; *Phy. Chem. Chem. Phys.* **2015**, *17*, 28484.
DOI: [10.1039/c5cp05212b](https://doi.org/10.1039/c5cp05212b)
- Welhama, N.; Berbennib, V.; Chapman, P.; *J. Alloy Compd*, **2003**, *349*, 255.
DOI: [10.1016/S0925-8388\(02\)00880-0](https://doi.org/10.1016/S0925-8388(02)00880-0)
- Huang, J.; *Acta Mater.* **1999**, *47*, 1801.
DOI: [10.1016/S1359-6454\(99\)00067-1](https://doi.org/10.1016/S1359-6454(99)00067-1)
- Chen, X.; Yang, H.; Wu, G.; Wang, M.; Deng, F.; Zhang, X.; *J. Cryst. Growth*, **2000**, *218*, 57.
DOI: [10.1016/S0022-0248\(00\)00486-3](https://doi.org/10.1016/S0022-0248(00)00486-3)
- Chun, H.; Li, L.; Kin, F.; George, W.; Tomy, F.; *Nature*, **2009**, *462*, 339.
DOI: [10.1038/nature08569](https://doi.org/10.1038/nature08569)

